Korean J Physiol Pharmacol 2024;28(4):303-312
https://doi.org/10.4196/kjpp.2024.28.4.303

KJPP

Original Article

Vinpocetine, a phosphodiesterase 1 inhibitor, mitigates atopic dermatitis-like skin inflammation

Yeon Jin Lee, Jin Yong Song, Su Hyun Lee, Yubin Lee, Kyu Teak Hwang, and Ji-Yun Lee*

Department of Pathophysiology, College of Pharmacy, Chung-Ang University, Seoul 06974, Korea

ARTICLE INFO

Received December 28, 2023
Revised February 1, 2024
Accepted February 3, 2024

***Correspondence**
Ji-Yun Lee
E-mail: jylee98@cau.ac.kr

Key Words
Atopic dermatitis
Dinitrochlorobenzene
Inflammation
Phosphodiesterase inhibitors
Transforming growth factor beta

ABSTRACT Atopic dermatitis (AD) is the most common inflammatory pruritic skin disease worldwide, characterized by the infiltration of multiple pathogenic T lymphocytes and histological symptoms such as epidermal and dermal thickening. This study aims to investigate the effect of vinpocetine (Vinp; a phosphodiesterase 1 inhibitor) on a 1-chloro-2,4-dinitrobenzene (DNCB)-induced AD-like model. DNCB (1%) was administered on day 1 in the AD model. Subsequently, from day 14 onward, mice in each group (Vinp-treated groups: 1 mg/kg and 2 mg/kg and dexamethasone-treated group: 2 mg/kg) were administered 100 μl of a specific drug daily, whereas 0.2% DNCB was administered every other day for 30 min over 14 days. The Vinp-treated groups showed improved Eczema Area and Severity Index scores and trans-epidermal water loss, indicating the efficacy of Vinp in improving AD and enhancing skin barrier function. Histological analysis further confirmed the reduction in hyperplasia of the epidermis and the infiltration of inflammatory cells, including macrophages, eosinophils, and mast cells, with Vinp treatment. Moreover, Vinp reduced serum concentrations of IgE, interleukin (IL)-6, IL-13, and monocyte chemotactic protein-1. The mRNA levels of IL-1β, IL-6, Thymic stromal lymphopoietin, and transforming growth factor-beta (TGF-β) were reduced by Vinp treatment. Reduction of TGF-β protein by Vinp in skin tissue was also observed. Collectively, our results underscore the effectiveness of Vinp in mitigating DNCB-induced AD by modulating the expression of various biomarkers. Consequently, Vinp is a promising therapeutic candidate for treating AD.

INTRODUCTION

Atopic dermatitis (AD) is a multifactorial skin disease involving innate and adaptive immune responses, influenced by complex genetic, pharmacological, and psychological factors [1]. AD is the most common chronic inflammatory skin disease, exhibiting diverse characteristics, such as impaired epidermal barrier, eczematous lesions, pruritus, and dry skin [2]. It also involves abnormal immune responses and an IgE-mediated allergy to various exogenous antigens [3,4]. AD is initiated by the release of cytokines (*e.g.*, thymic stromal lymphopoietin [TSLP] and interleukin [IL]-1β, IL-25, and IL-33) that activate Langerhans cells in response to allergen exposure to keratinocytes [5]. TSLP plays a central role in differentiating naïve helper T cells into type 2 helper T (Th2) cells, which are key contributors to AD symptoms [6]. Activated Langerhans cells stimulate Th2 cells, inducing the production of cytokines (IL-4, IL-5, IL-13, IL-31, and IL-33) resulting in symptoms such as barrier dysfunction, impaired keratinocyte differentiation, and itching [7]. Additionally, chronic AD is characterized by the recruitment of the Th1, Th22, and Th17 subsets, leading to abnormal keratinocyte proliferation and epidermal thickening [8]. To date, steroid ointments or creams are commonly used for treating AD and provide rapid relief; however, the symptoms are exacerbated upon discontinuation

Author contributions: Y.J.L. and J.Y.L. designed the study. Y.J.L. and J.Y.S. wrote the manuscript, performed animal experiments, and analyzed the data. Y.J.L., S.H.L., Y.L., and K.T.H. measured cytokines level. J.Y.S. revised the manuscript and performed Western blotting. J.Y.L. supervised and coordinated the study.

[9]. In addition, small-molecule drugs that control various physiological responses with fewer side effects have been developed [10]. Phosphodiesterases (PDEs) consist of 11 subtypes (PDE 1–11) and more than 40 isoforms [11]. PDEs catalyze the hydrolysis of cyclic adenosine monophosphate (cAMP) and guanosine monophosphate (GMP), regulating the intracellular concentration of these cyclic nucleotides [12]. A PDE 4 inhibitor blocks the hydrolysis of cAMP, increases intracellular cAMP, and sequentially activates protein kinase A, cAMP-response element-binding protein [13]. This leads to the inhibition of nuclear factor kappa B and nuclear factor-activated T cells, suppressing the secretion of related cytokines [14]. It regulates and reduces the skin inflammatory response occurring in AD [15]. Eucrisa is an example of a PDE 4 inhibitor drug, which is not currently utilized in Korea [16]. cAMP is a ubiquitous secondary messenger in the cells of all biological systems, controlling vital actions such as cell proliferation, cardiac function, and memory in mammalian cells [17,18]. Elevated cAMP levels induce relaxation in airway smooth muscle and inhibit various immune and inflammatory responses [19]. These responses are fundamental in asthma, including the activation and proliferation of T lymphocytes, the production of superoxide anions in eosinophils, and the chemotaxis of eosinophils stimulated by inflammatory mediators [20,21]. PDE inhibitors, crucial in the metabolism of cAMP and cyclic GMP, modulate the release of inflammatory cytokines as intracellular secondary messengers [22]. Vinpocetine (Vinp), a PDE 1 inhibitor and derivative of the alkaloid vincamine, has been clinically employed for over 30 years to address cerebrovascular disorders such as dementia and stroke [23]. Numerous studies have explored the anti-inflammatory effects of Vinp, revealing its ability to inhibit IκB kinase as a key mechanism [24]. Previous research has demonstrated the efficacy of Vinp in mitigating ovalbumin (OVA)-induced asthma [25], with subsequent studies further confirming its effects [26]. Furthermore, the impact of Vinp was investigated using diverse pathophysiological data in a 2,4-Dinitrochlorobenzene (DNCB)-induced AD model. This study aimed to investigate the effect of Vinp on DNCB-induced AD-like model. Our findings may help evaluate the effectiveness of Vinp in mitigating DNCB-induced AD. Consequently, we have shown that Vinp has great potential to be developed as an AD treatment.

METHODS

Materials

DNCB (cat no. 237329) and water-soluble dexamethasone (Dex; BioReagent, cat no. D2915), avertin (2,2,2-tribromoethanol, T48402), and acetone (suitable for HPLC, ≥ 99.9%) were obtained from Sigma-Aldrich. Vinp was purchased from TCI, and olive oil was sourced from DAEJUNG.

Animals

Four-week-old female Balb/c mice were purchased from Young Bio. Mice were housed in a controlled animal facility at Chung-Ang University with a temperature of 24°C ± 2°C, humidity at 50% ± 5%, and a 12-h light–dark cycle for 7 days. The mice were randomly divided into five groups (n = 5 or 6): (1) control, (2) DNCB, (3) DNCB + Vinp 1 mg/kg, (4) DNCB + Vinp 2 mg/kg, and (5) DNCB + Dex 2 mg/kg. Animal studies were conducted in accordance with the ethical guidelines and regulations established by the Institutional Animal Care and Use Committee of Chung-Ang University (approval number IACUC-202211010010).

DNCB-induced model for AD

All mice, except those in the control group, were sprayed with 1% DNCB through a vehicle (acetone:olive oil = 4:1) on their dorsal skin on day 1. The backs of the mice were shaved the day before the first day of the experiment. In the control group, the vehicle was applied to the dorsal skin. Starting from day 14, each mouse was topically administered 100 μl of a specific drug daily (1 mg/kg Vinp; 2 mg/kg Vinp; or 2 mg/kg Dex through a vehicle). Additionally, 0.2% DNCB was administered every other day for 30 min over a 14-day period. On day 28, all mice were sacrificed, and serum and dorsal skin samples were collected after measuring the trans-epidermal water loss (TEWL) from the dorsal skin (Fig. 1A).

Evaluation of dermatitis

The severity of dermatitis was determined using the modified Eczema Area and Severity Index (EASI) on day 28, which assesses the degree of four symptoms (erythema, edema, excoriation, and lichenification) as follows: 0 = absent, 1 = mild, 2 = moderate, and 3 = severe. The dermatitis score was calculated by summing these four scores. In the control group, the vehicle was applied to the dorsal skin.

Hematoxylin & eosin (H&E) staining

H&E staining was performed by referring to a previous description [27]. For histological analysis, dorsal skin tissue was fixed in 4% formaldehyde, embedded in paraffin using the Tissue-Tek TEC 5 Tissue Embedding Console System from Sakura Finetek, Torrance, and sliced into 4-μm sections. Subsequently, dorsal skin specimens were deparaffinized at 60°C for 15 min and then stained with H&E. Images of the stained dorsal skin specimens were captured using a Leica DM 480 camera (Leica Microsystems). The epidermis and dermis thicknesses were measured using the ImageJ software.

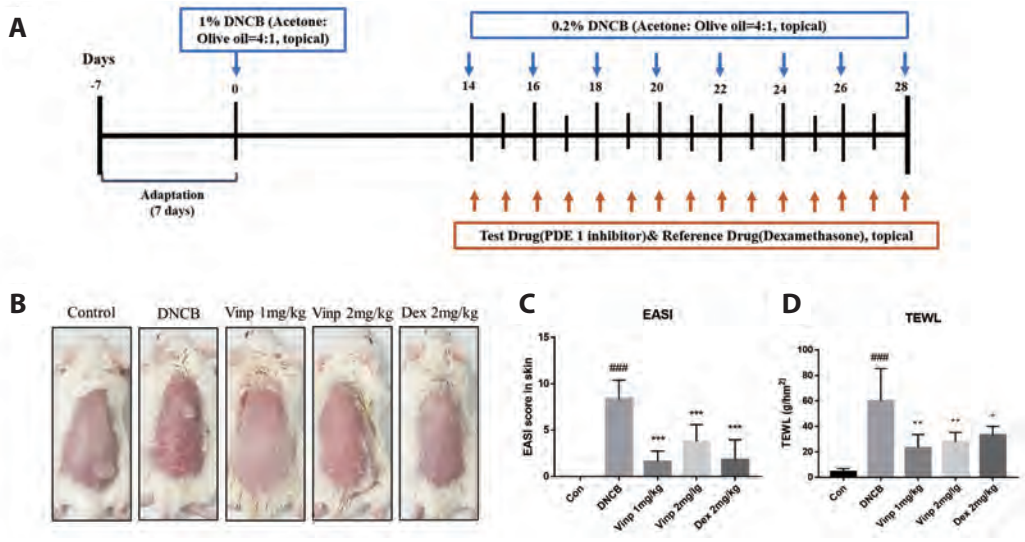

Fig. 1. Experimental schedule and effect of Vinp on clinical changes in DNCB-induced AD. (A) Experimental schedule for DNCB-induced AD. (B) Representative images showing control and DNCB-induced AD mice treated with vehicle, Vinp at 1 mg/kg and 2 mg/kg, and Dex at 2 mg/kg. (C) Each region was separately assessed for four signs based on the EASI score: erythema, edema, excoriation, and lichenification. Each sign was assigned an intensity score from 0 to 3, with 0 indicating absence; 1: mild; 2: moderate; and 3: severe. Scores were evaluated through macroscopic observations. (D) TEWL levels in Balb/c dorsal skin were measured to assess the degree of moisture loss in the skin on the last day of the experiment (day 28). Data represent means ± SD (n = 5 or 6). Statistical analysis was performed using one-way ANOVA (Data were considered significant at $^{###}p < 0.001$ compared with the control group and $^{*}p < 0.1$, $^{**}p < 0.01$, $^{***}p < 0.001$ compared with the DNCB group). AD, atopic dermatitis; DNCB, 1-chloro-2,4-dinitrobenzene; Vinp, vinpocetine; Dex, dexamethasone; EASI, eczema area and severity index; TEWL, transepidermal water loss; PDE, phosphodiesterase.

Immunohistochemistry (IHC)

For IHC, dorsal skin specimens were deparaffinized at 60°C for 2 h, and rehydrated in a series of alcohol solutions, and finally in distilled water. Subsequently, the cross-linked antigens of the specimens were lysed using an antigen retrieval solution (Dako). Following the blocking of endogenous peroxidase with 3% hydrogen peroxide, immune cells and macrophages were identified using anti-CD45 antibody, anti-F4/80 antibody (CST), and the Vectastain Elite ABC kit (c). Staining of the specimens was performed using a DAB substrate kit (Vector Laboratories) and hematoxylin. Images of the stained dorsal skin specimens were captured using a Leica DM 480 camera (Leica Microsystems). The degree of immune cells and macrophage infiltration was evaluated by comparing the stained area to the total area using ImageJ software.

Congo red staining

Dorsal skin samples were deparaffinized at 60°C for 15 min and subsequently stained with a Congo red staining kit (Abcam). Images of the stained dorsal skin samples were captured using a Leica DM 480 camera (Leica Microsystems). The degree of mast cell infiltration was evaluated by counting red-stained eosinophils in the observed fields using ImageJ software.

Toluidine blue staining

The dorsal skin specimens were deparaffinized at 60°C for 15 min, followed by staining with toluidine blue to facilitate the observation of infiltrated mast cells. Images of the stained dorsal skin specimens were captured using a Leica DM 480 camera (Leica Microsystems). The degree of mast cell infiltration was evaluated by counting the blue-stained mast cells in the field using ImageJ software for analysis.

Western blot analysis

The protein levels in the skin tissues were assessed through Western blot analysis. Western blot analysis was performed by referring to a previous description [28]. The primary antibodies used were anti-TGF-β antibody (cat no. A2124; ABclonal) and anti-GAPDH antibody (cat no. A19056; ABclonal). An HRP-linked anti-rabbit IgG (cat no. 31460; Invitrogen) was used as secondary antibody. Four mouse samples were used in each group (Supplementary Fig. 1).

Enzyme-linked immunosorbent assay (ELISA)

Serum samples were collected by centrifuging blood at 1,500 g and for 10 min at 4°C and subsequently stored at −80°C. The levels of IgE, IL-6, and IL-13 in the serum were measured using an IgE ELISA kit (BD) and a colorimetric sandwich ELISA kit

(Quantikine ELISA; R&D Systems). The absorbance was measured using a Synergy HTX multimode plate reader (BioTek).

Quantitative reverse transcription PCR (RT-qPCR)

RT-qPCR was performed to assess mRNA expression levels. Total RNAs were extracted using TRIzol reagent (Ambion; Life Technologies) and quantified spectrophotometrically with NanoDrop ND-1000 (Thermo Fisher Scientific). Subsequently, cDNA was synthesized from 1 μg of RNA using the iScript cDNA synthesis kit (Bio-Rad). The target cDNA was then amplified using specific primers and iQ SYBR Green Supermix (Bio-Rad). The initial denaturation of cDNA occurred at 95°C for 3 min, followed by 40 cycles of denaturation (at 95°C for 10 sec), annealing (at 55°C for 30 sec), and plate reading. Post-cycling, a melting curve was generated by increasing the temperature from 55 to 95°C, with a plate read at each step-up. The CFX96 Real-Time PCR Detection System (Bio-Rad) was used, and the CFX Manager software automatically determined the cycle quantification value at which samples exhibited a sufficiently high signal (ΔC_T values). Each ΔC_T value was normalized against *GAPDH*, which served as a housekeeping gene. Transcript expression levels were then determined relative to those of the control group. The RT-qPCR analysis was replicated in three independent experiments (n = 5 or 6).

Statistical analysis

All values are presented as a mean ± standard deviation of data (n = 5). Statistical analyses were performed using one-way analysis of variance (ANOVA). Differences among the groups were considered statistically significant at $p < 0.05$. Significant differences compared with control group are marked by hash ($^{\#}p < 0.05$, $^{\#\#}p < 0.01$, $^{\#\#\#}p < 0.001$). Significant differences compared with DNCB group are marked by asterisk mark (*p < 0.05, **p < 0.01, ***p < 0.001).

RESULTS

Effects of Vinp on DNCB-induced AD in BALB/c mice

To evaluate the effects of Vinp on the DNCB-induced AD-like model, we conducted skin assessments, analyzed EASI score, and measured TEWL. On day 28, we captured images of the dorsal skin of mice. Notably, DNCB-induced AD was alleviated in the Vinp 1 mg/kg, Vinp 2 mg/kg, and Dex 2 mg/kg groups (Fig. 1B). The severity of AD was evaluated using the EASI. The EASI score was significantly higher in the DNCB-induced AD group (8.33 ± 1.89) ($^{\#\#\#}p < 0.001$) compared with the control group (0 ± 0). Notably, in Vinp 1 mg/kg (1.60 ± 1.02) (***p < 0.001), Vinp 2 mg/kg (3.80 ± 1.60) (***p < 0.001), and Dex 2 mg/kg (1.80 ± 1.94) (***p < 0.001) groups, the EASI score showed a marked attenuation (Fig. 1C). To assess TEWL, measurements were taken immediately before sacrifice. TEWL levels were significantly increased in the DNCB group (60 ± 23.12 g/hm^2) ($^{\#\#\#}p < 0.001$) compared with the control group (4.2 ± 2.4 g/hm^2). The Dex 2 mg/kg group showed a significant reduction in TEWL (33 ± 6.2312 g/hm^2) (**p < 0.01). In particular, the TEWL levels were remarkably decreased in the Vinp 1 mg/kg (23 ± 9.44 g/hm^2) (**p < 0.01) and Vinp 2 mg/kg (27.6 ± 6.83 g/hm^2) (**p < 0.01) groups (Fig. 1D).

Effects of Vinp on pathohistological changes in atopic-dermatitis model skin tissues

H&E staining was performed to visualize epidermal and dermal hyperplasia. Significant histological changes were observed in the dorsal skin specimens stained with H&E (Fig. 2A). The epidermal thickness in the DNCB group (62.23 ± 12.18 μm) ($^{\#\#\#}p < 0.001$) was significantly higher compared with the control group (18.34 ± 1.98 μm). The epidermal hyperplasia induced by DNCB was remarkably improved in the Vinp 1 mg/kg (36.35 ± 6.38 μm) (***p < 0.001) and Vinp 2 mg/kg (41.22 ± 4.75 μm) (**p < 0.01) groups. In the Dex 2 mg/kg group, epidermal hyperplasia also exhibited improvement, showing a reduction by 35.55 ± 6.51 μm (***p < 0.001) (Fig. 2B). A similar pattern was observed for dermal thickness. In the DNCB group (36.24 ± 3.82 μm) ($^{\#\#\#}p < 0.001$), dermal thickness significantly increased compared with the control group (19.98 ± 2.92 μm). Remarkably, in the Vinp 1 mg/kg and Vinp 2 mg/kg groups, dermal thicknesses were reduced by 28.62 ± 1.54 μm (***p < 0.001), and 24.57 ± 4.91 μm (**p < 0.01), respectively (Fig. 2C).

Effect of Vinp on infiltration of immune cells and macrophages in skin tissues

IHC analyses of CD45 and F4/80 were conducted to identify immune cells and macrophages in dorsal skin tissues. The infiltration of immune cells and macrophages was evaluated by calculating the ratio of the CD45- or F4/80-positive area to the total area. In the DNCB-induced mice group, CD45$^+$ cells occupied 18.7% ± 4.09% of the area, indicating a significant difference compared with the control group, in which CD45$^+$ cells occupied 7.7% ± 1.33% of the area ($^{\#\#\#}p < 0.001$). In contrast, the area occupied by CD45$^+$ cells decreased in both the Vinp 1 mg/kg (14.33% ± 2.50%) (**p < 0.01) and Vinp 2 mg/kg (14.94% ± 1.81%) (**p < 0.01) groups. The reference drug, Dex 2 mg/kg, exhibited a slightly more pronounced decrease (11.52% ± 2.03%) (***p < 0.001) (Fig. 3A, B). Furthermore, F4/80+ cells occupied 15.39% ± 6.35% of the area in the DNCB group, indicating a remarkable difference compared with the control group, in which F4/80$^+$ cells occupied 1.98% ± 0.60% of the area ($^{\#\#\#}p < 0.001$). Both the Vinp 1 mg/kg (3.62% ± 1.00%) (***p < 0.001) and Vinp 2 mg/kg (2.92% ± 0.61%) (***p < 0.001) groups showed a similar decrease in the infiltration

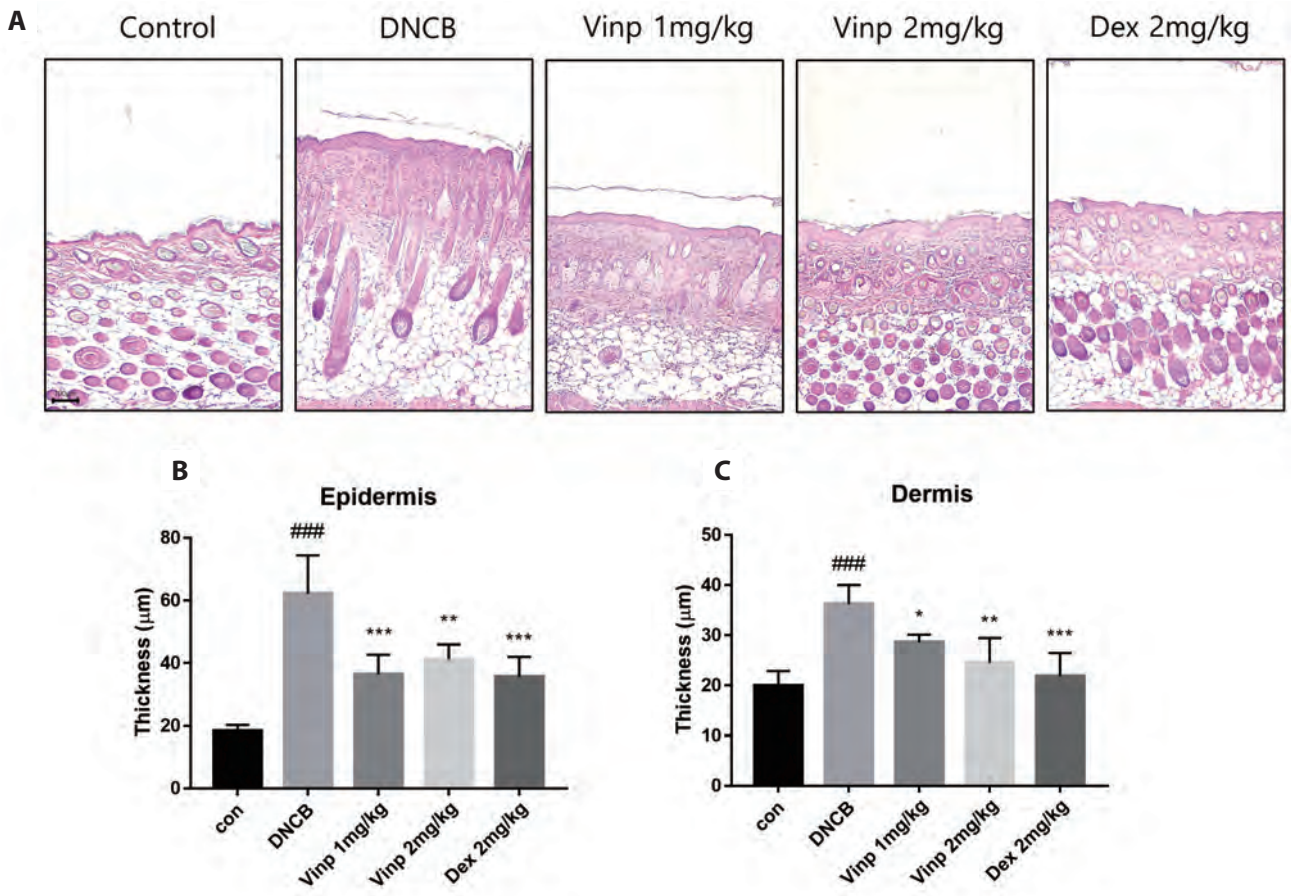

Fig. 2. Effect of Vinp on the thickness of dorsal skin tissue. (A) H&E staining was performed to investigate the changes in epidermal and dermal hyperplasia. To evaluate the effect of Vinp on DNCB-induced skin lesions, DNCB was repeatedly applied to the dorsal skin of Balb/c mice (left hand side: magnification 100×; scale bar: 100 μm). (B) DNCB application increased epidermal thickness by 3.39-fold compared with the control group. (C) DNCB application increased dermal thickness by 1.81-fold compared with the control group. However, Vinp treatment significantly inhibited DNCB-induced increases in epidermal and dermal thickness. Data represent means ± SD (n = 5 or 6). Data were considered significant at $^{###}p < 0.001$ compared with the control group and *p < 0.1, **p < 0.01, ***p < 0.001 compared with the DNCB group. DNCB, 1-chloro-2,4-dinitrobenzene; Vinp, vinpocetine; Dex, dexamethasone.

of F4/80$^+$ cells. Similarly, in the Dex 2 mg/kg group, the infiltration of F4/80$^+$ cells decreased significantly (0.97% ± 0.14%) (***p < 0.001) (Fig. 3C, D).

Effect of Vinp on infiltration of allergic inflammatory cells into the skin

Congo red and toluidine blue staining were performed to investigate the infiltration of eosinophils and mast cells into the dorsal skin, respectively. The number of eosinophils was significantly increased in the DNCB group (8.74 ± 0.85) ($^{###}p < 0.001$). Subsequently, eosinophil infiltration was significantly decreased in the Vinp 1 mg/kg group (4.92 ± 0.94) (**p < 0.01), and a similar effect was observed in the Vinp 2 mg/kg group (4.67 ± 1.44) (**p < 0.01). Additionally, a notable reduction in eosinophils infiltration was evident in the Dex-treated group (3.90 ± 1.62) (***p < 0.001) (Fig. 4A, B). Additionally, toluidine blue staining revealed a significant increase in the number of mast cells in the DNCB group (20.92 ± 3.28) ($^{###}p < 0.001$) compared with the control group (1.84 ± 0.57). In the Vinp 1 mg/kg group, mast cells were markedly reduced in skin tissues (11.45 ± 2.35) (***p < 0.001). This reduction in the number of mast cells was also observed in the Vinp 2 mg/kg (12.31 ± 2.69) (**p < 0.01) and Dex-treated (7.78 ± 0.73) (***p < 0.001) groups (Fig. 4C, D).

Effect of Vinp on allergic inflammatory biomarkers in serum

Immunoglobulin levels were analyzed using ELISA to examine the degree of systemic allergy and inflammation. IgE levels were notably increased in the DNCB group (1,765.20 ± 108.74 pg/ml) ($^{###}p < 0.001$) compared with the control group (115.55 ± 6.77 pg/ml). In contrast, IgE levels significantly decreased in the Vinp 1 mg/kg (999.03 ± 140.0 pg/ml) (**p < 0.01), Vinp 2 mg/kg (1,096.10

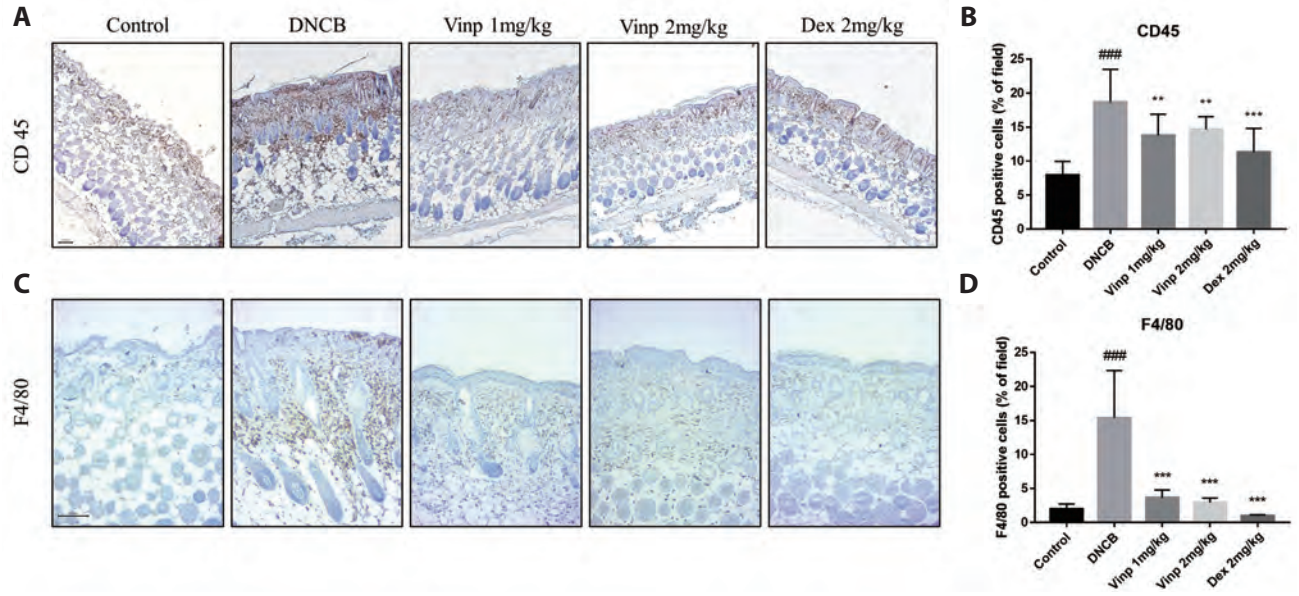

Fig. 3. Effect of Vinp on the infiltration of immune cells. The effect of Vinp on immune cell infiltration and the numbers of (A) $CD45^+$ and (C) $F4/80^+$ cells in the DNCB-induced AD model were analyzed using IHC staining (left hand side: $CD45^+$: magnification 100×, $F4/80^+$: magnification 200×; scale bar: 100 μm). (B) $CD45^+$ and (D) $F4/80^+$ cells were examined for immune cell and macrophage infiltration and counted using ImageJ software. Data represent means ± SD (n = 5 or 6). Data were considered significant at $^{###}p < 0.001$ compared with the control group and $^{**}p < 0.01$ and $^{***}p < 0.001$ compared with the DNCB group. IHC, immunohistochemistry; DNCB, 1-chloro-2,4-dinitrobenzene; Vinp, vinpocetine; Dex, dexamethasone; AD, atopic dermatitis.

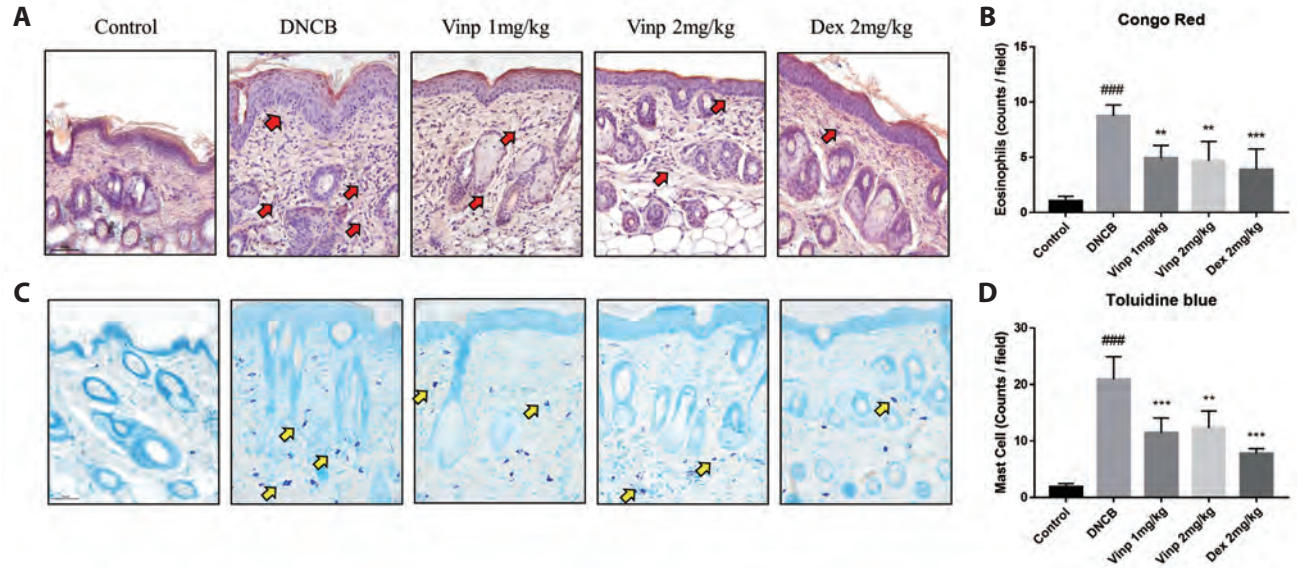

Fig. 4. Effect of Vinp on the infiltration of eosinophils and mast cells into the skin. (A) Congo red and (C) Toluidine blue staining procedures were used to identify eosinophils and mast cells. Red and yellow arrows indicate the Congo red-stained eosinophils and mast cells, respectively (left hand side: magnification 400×; scale bar: 100 μm). (B) Eosinophils and (D) mast cells were counted using ImageJ software. Data represent mean ± SD (n = 5 or 6). Data were considered significant at $^{###}p < 0.001$ compared with the control group and $^{**}p < 0.01$ and $^{***}p < 0.001$ compared with the DNCB group. DNCB, 1-chloro-2,4-dinitrobenzene; Vinp, vinpocetine; Dex, dexamethasone.

± 78.26 pg/ml) ($^{**}p < 0.01$), and Dex-treated (986.55 ± 272.74 pg/ml) ($^{**}p < 0.01$) groups compared with the DNCB group (Fig. 5A). The increase in IL-13 among Th2 cytokines in acute lesions of AD was investigated using an ELISA kit. IL-13 levels significantly increased in the DNCB group (213.24 ± 48.37 ng/ml) ($^{###}p < 0.001$) compared with the control group (95.59 ± 37.59 ng/ml). Further, in the Vinp 2 mg/kg group, the IL-13 level in serum was significantly reduced compared with the DNCB group (146.80

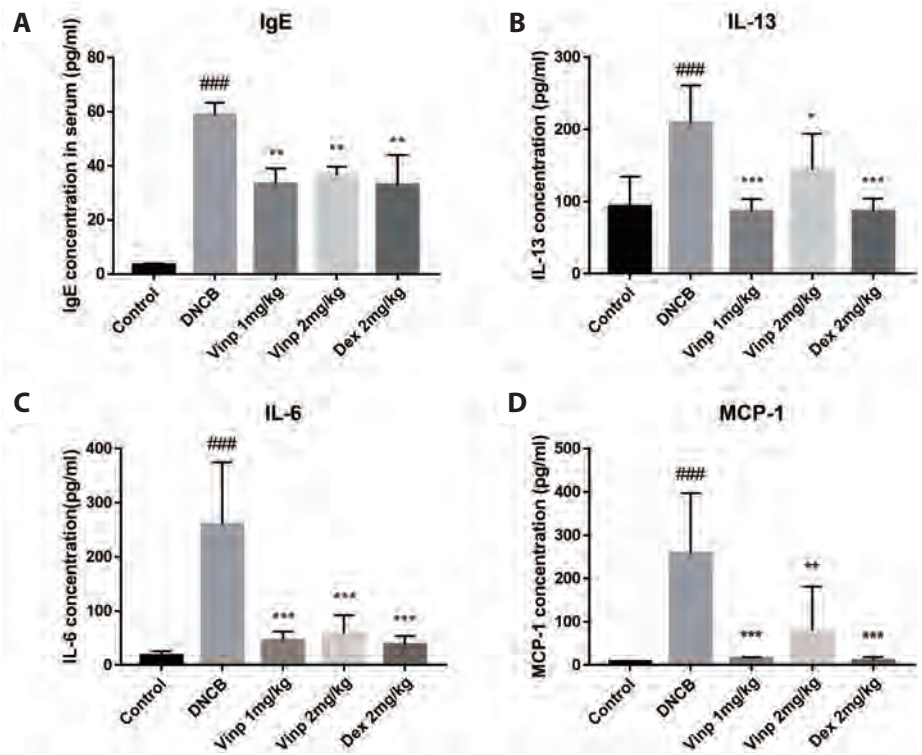

Fig. 5. Effect of Vinp on the IgE, IL-13, IL-6, MCP-1 concentrations in serum. (A) IgE, (B) IL-13, (C) IL-6, (D) MCP-1 levels in serum were measured using ELISA kits (n = 5 or 6). All values are presented as mean ± SD. Data were considered significant at $^{###}p < 0.001$ compared with the control group and *p < 0.1, **p < 0.01, and ***p < 0.001 compared with the DNCB group. Ig, immunoglobulin; IL, interleukin; MCP, monocyte chemoattracted protein; ELISA, enzyme-linked immunosorbent assay; DNCB, 1-chloro-2,4-dinitrobenzene; Vinp, vinpocetine; Dex, dexamethasone.

± 45.70 ng/ml) (*p < 0.05). Notably, a substantial decrease in IL-13 level was observed in the Vinp 1 mg/kg (87.98 ± 15.96 ng/ml) (***p < 0.001) and Dex-treated (87.98 ± 16.47 ng/ml) (***p < 0.001) groups (Fig. 5B). Serum IL-6 levels were measured to determine the effects of Vinp on the release of inflammatory cytokines. The IL-6 levels were significantly increased in the DNCB group (259.47 ± 105.35 ng/ml) ($^{###}p < 0.001$) compared with the control group (17.20 ± 7.05 ng/ml). In particular, IL-6 levels were remarkably decreased in the Vinp 1 mg/kg (45.73 ± 14.55 ng/ml) (***p < 0.001) and Vinp 2 mg/kg (58.23 ± 30.44 ng/ml) (***p < 0.001) groups. The increase in IL-6 level induced by DNCB was also significantly reduced in the Dex-treated group (37.26 ± 14.28 ng/ml) (***p < 0.001) (Fig. 5C). Monocyte chemotactic protein-1 (MCP-1) levels in serum significantly increased in the DNCB group (25.80 ± 14.55 pg/ml) ($^{###}p < 0.001$) compared with the control group (0.73 ± 14.55 pg/ml). In the Vinp 2 mg/kg group, MCP-1 level in the serum was significantly decreased compared with the DNCB group (8.00 ± 9.06 pg/ml) (**p < 0.01). Notably, the MCP-1 level was reduced in the Vinp 1 mg/kg (1.47 ± 0.32 pg/ml) (***p < 0.001) and Dex-treated (1.00 ± 0.75 pg/ml) (***p < 0.001) groups (Fig. 5D).

Effect of Vinp on expression of cytokines in skin tissue

The mRNA levels of IL-1β, IL-6, IL-4, TSLP, and TGF-β were analyzed using qPCR to investigate the impact of Vinp on cytokine production in skin tissues. Specifically, IL-1β and IL-6 mRNA expressions were analyzed to examine cytokines associated with eosinophil infiltration through RT-qPCR. Notably, the IL-1β mRNA expression significantly increased in the DNCB group (7.73 ± 2.72-fold compared with the control) ($^{###}p < 0.001$). In contrast, the IL-1β mRNA expression significantly decreased in the Vinp 1 mg/kg (3.36 ± 0.93-fold compared with the control) (**p < 0.01), Vinp 2 mg/kg (3.99 ± 1.90-fold compared with the control) (**p < 0.01), and Dex-treated (0.84 ± 0.37-fold compared with the control) (***p < 0.001) groups (Fig. 6A). Similarly, the IL-6 mRNA expression increased in the DNCB group (5.72 ± 3.83-fold compared with the control) ($^{##}p < 0.01$). However, IL-6 expression significantly decreased in the Vinp 1 mg/kg (2.43 ± 1.08) (**p < 0.01), Vinp 2 mg/kg (2.38 ± 0.88) (*p < 0.05), and Dex-treated (1.05 ± 0.70-fold compared with the control) (**p < 0.01) groups (Fig. 6B). TSLP levels were analyzed to examine cytokine-related to Th2 cell differentiation, and they were significantly higher in the DNCB group (8.80 ± 1.40-fold compared with the control) ($^{##}p < 0.01$). In contrast, the increase in TSLP expression was significantly inhibited in the Vinp 1 mg/kg (2.29 ± 0.32-fold compared with the control) (**p < 0.01), Vinp 2 mg/kg (2.06 ± 1.01-fold compared with the control) (**p < 0.01), and Dex-treated (3.60 ± 2.09-fold compared with the control) (*p < 0.5) groups (Fig. 6C). Furthermore, the mRNA level of IL-4 was increased in the skin tissues of the DNCB group (2.35 ± 0.62-fold compared with the control). The upregulation of IL-4 expression induced by DNCB was reduced in the Vinp 1 mg/kg (1.06 ± 0.25-fold compared with the control) (*p < 0.05) and Dex-treated (1.08 ± 0.70-fold compared with the control) (*p < 0.05) groups. Unfortunately, no significant difference was observed between the DNCB and Vinp 2 mg/kg (1.89 ± 0.98-fold compared with the control)

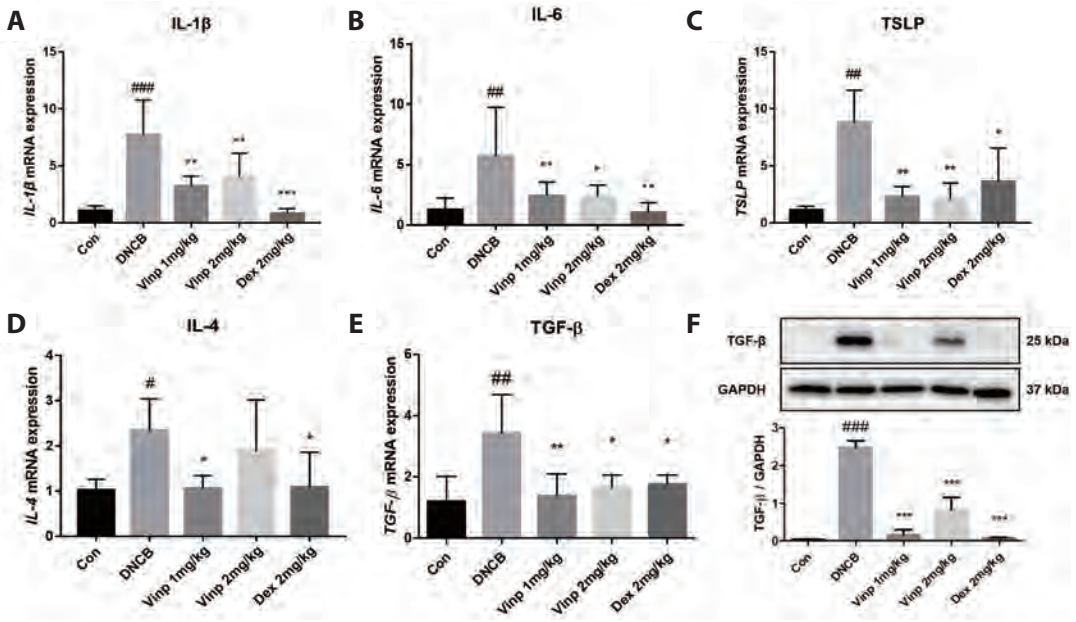

Fig. 6. Effects of Vinp on the expression of inflammatory cytokines in skin tissue. (A–E) mRNA expression levels of IL-1β, IL-6, IL-4, TSLP, and TGF-β, respectively (n = 5 or 6). All values are presented as mean ± SD. (F) TGF-β protein levels in skin tissues were observed using Western blot (n = 4). Data were considered significant at $^{\#}p < 0.1$, $^{\#\#}p < 0.01$, $^{\#\#\#}p < 0.001$ compared with the control group and $^{*}p < 0.1$, $^{**}p < 0.01$, $^{***}p < 0.001$ compared with the DNCB group. IL, interleukin; TSLP, thymic stromal lymphopoietin; TGF, transforming growth factor; GAPDH, glyceraldehyde 3-phosphate dehydrogenase; DNCB, 1-chloro-2,4-dinitrobenzene; Vinp, vinpocetine; Dex, dexamethasone.

groups (Fig. 6D). Additionally, TGF-β levels were analyzed to investigate changes in a cytokine related to the effect on skin barrier recovery, and they were found to be significantly increased in the DNCB group (3.43 ± 1.12-fold compared with the control) ($^{\#\#}p < 0.01$). Both Vinp 1 mg/kg and Vinp 2 mg/kg groups showed a similar decrease in TGF-β expression (1.38 ± 0.64; $^{**}p < 0.01$, 1.66 ± 0.36; $^{*}p < 0.05$-fold compared with the control). Moreover, the increase in TGF-β expression was inhibited in the Dex-treated group (1.05 ± 0.70-fold compared with the control) ($^{*}p < 0.05$) (Fig. 6E). The protein levels of TGF-β were decreased in Vinp 1 mg/kg, Vinp 2 mg/kg, and Dex-treated groups (0.15 ± 0.13; $^{***}p < 0.001$, 0.83 ± 0.31; $^{***}p < 0.001$, 0.07 ± 0.02; $^{***}p < 0.001$) increased by DNCB (2.48 ± 0.18; $^{\#\#\#}p < 0.001$) (Fig. 6F).

DISCUSSION

In a previous study using an OVA-induced AD model, the effect of Vinp was explored through oral (20 mg/kg), intraperitoneal (10 mg/kg), and topical (2 mg/kg) administration. Notably, topical administration was reported as the most effective [26]. As topical administration allows for significantly smaller doses, it may have a beneficial effect on AD, particularly during long-term treatment [29]. However, studies on the improvement of AD pathophysiology using Vinp are lacking. Therefore, in this study, the effect of Vinp was investigated with a focus on topical administration based on pathophysiological data.

Patients with AD exhibit thick and darkened skin due to the recurrence and continuation of severe itching, leading to redness, rash formation on wounds, and the development of scabs [30]. Although the exact etiology remains unclear, AD is a multifactorial skin condition influenced by genetic factors, immunological abnormalities, and environmental changes that interact in a complex manner [31]. The onset is predominately during infancy [32], with spontaneous resolution typically occurring by the age of seven; however, some cases may persist into adulthood [33]. Between 2012 and 2020, an average of approximately 940,000 patients received treatment for AD in Korea annually, with a higher prevalence among those under the age of nine. Notably, the incidence tends to decrease with age [34]. In contrast to pediatric cases, adult patients with AD exhibit an increasing trend in symptoms, indicating that acute symptoms are frequently accompanied by continuous chronic symptoms [35].

The degree of AD can be assessed using EASI and evaluating barrier dysfunction [36]. In this study, we evaluated barrier dysfunction by measuring TEWL. The EASI score, employed in our study, evaluates severity. Specifically, redness (erythema),inflammation, thickness (induration), papulation, swelling indicative of acute eczema, scratching (excoriation), and lichenification (lined skin, furrowing, and prurigo nodules for chronic eczema) across the neck, upper legs, lower legs, and trunk are evaluated [37]. To evaluate the degree of AD in the mice, we applied a modified EASI score, focusing exclusively on dorsal skin lesions. Patients with AD often experience barrier dysfunc-

tion due to various factors, including genetic predisposition and environmental influences such as filaggrin mutations and the itch-scratch cycle [38].

Vinp improved the EASI and TEWL scores, which implies that Vinp improved the clinical signs of AD and the skin barrier. The epidermal hyperplasia is characterized in various skin inflammation such as AD and psoriasis [2,39]. The H&E staining revealed a reduction in epidermal and dermal hyperplasia induced by DNCB in the Vinp-treated groups. This suppression of overgrowth appears to be associated with decreased TGF-β production, as confirmed using qRT-PCR and Western blot in Fig. 6.

Our findings demonstrated that Vinp influenced the infiltration of various inflammatory cells. CD45 serves as a surface marker for immune cells, whereas F4/80 is a marker of the monocyte–macrophage transition [40,41]. Eosinophils are increased in the serum and skin lesions of patients with AD, activated by the Th2 cytokine IL-5. The number of infiltrating eosinophils in tissues correlates with AD severity [42]. Mast cells are white blood cells that mainly cause the allergies [43] and contain histamine granules. When IgE is conjugated to the FcεRI of mast cells, histamine is released through degranulation [44]. Our histological data revealed that Vinp decreased inflammation by reducing the recruitment of inflammatory cells. In addition, ELISA confirmed the improvement in AD. Vinp decreased the serum concentration of IgE, which induces mast cell activation. Vinp reduced the serum levels of IL-6, IL-13, and MCP-1. It also reduced mRNA expression levels of TSLP, IL-1β, IL-6, IL-4.

In conclusion, Vinp improved dermatitis, skin water loss, and serum IgE levels, and inhibited inflammatory cell infiltration and epidermal hyperplasia in the skin by regulating the expression of various biomarkers, such as IL-6, IL-13, and MCP-1. Vinp's positive impact on dermatitis, skin water loss, and inflammatory markers suggests its therapeutic potential for AD. These findings have implications for developing novel treatments targeting specific disease biomarkers, opening avenues for advanced therapeutic strategies. Deeper exploration of molecular mechanisms affected by Vinp, understanding its long-term effects on disease progression, and examining its clinical application potential are vital areas for future investigation to advance this study.

FUNDING

This research was supported by the Chung-Ang University Research Scholarship Grants in 2022.

ACKNOWLEDGEMENTS

None.

CONFLICTS OF INTEREST

The authors declare no conflicts of interest.

SUPPLEMENTARY MATERIALS

Supplementary data including one figure can be found with this article online at https://doi.org/10.4196/kjpp.2024.28.4.303

REFERENCES

1. Magnifico I, Petronio Petronio G, Venditti N, Cutuli MA, Pietrangelo L, Vergalito F, Mangano K, Zella D, Di Marco R. Atopic dermatitis as a multifactorial skin disorder. Can the analysis of pathophysiological targets represent the winning therapeutic strategy? *Pharmaceuticals (Basel).* 2020;13:411.
2. Lee J, Park L, Kim H, Rho BI, Han RT, Kim S, Kim HJ, Na HS, Back SK. Adipose-derived stem cells decolonize skin *Staphylococcus aureus* by enhancing phagocytic activity of peripheral blood mononuclear cells in the atopic rats. *Korean J Physiol Pharmacol*. 2022;26:287-295.
3. Kim BE, Leung DY. Epidermal barrier in atopic dermatitis. *Allergy Asthma Immunol Res*. 2012;4:12-16.
4. Lee HJ, Lee SH. Epidermal permeability barrier defects and barrier repair therapy in atopic dermatitis. *Allergy Asthma Immunol Res*. 2014;6:276-287.
5. Fania L, Moretta G, Antonelli F, Scala E, Abeni D, Albanesi C, Madonna S. Multiple roles for cytokines in atopic dermatitis: from pathogenic mediators to endotype-specific biomarkers to therapeutic targets. *Int J Mol Sci*. 2022;23:2684.
6. Akdis CA, Arkwright PD, Brüggen MC, Busse W, Gadina M, Guttman-Yassky E, Kabashima K, Mitamura Y, Vian L, Wu J, Palomares O. Type 2 immunity in the skin and lungs. *Allergy*. 2020;75:1582-1605.
7. Haddad EB, Cyr SL, Arima K, McDonald RA, Levit NA, Nestle FO. Current and emerging strategies to inhibit type 2 inflammation in atopic dermatitis. *Dermatol Ther (Heidelb)*. 2022;12:1501-1533.
8. Biedermann T, Skabytska Y, Kaesler S, Volz T. Regulation of T cell immunity in atopic dermatitis by microbes: the Yin and Yang of cutaneous inflammation. *Front Immunol*. 2015;6:353.
9. Kim JM, Park SH. Risk and benefit of steroid therapy. *Korean J Med*. 2009;77:298-303.
10. Worm M, Francuzik W, Kraft M, Alexiou A. Modern therapies in atopic dermatitis: biologics and small molecule drugs. *J Dtsch Dermatol Ges*. 2020;18:1085-1092.
11. Bollen E, Prickaerts J. Phosphodiesterases in neurodegenerative disorders. *IUBMB Life*. 2012;64:965-970.
12. Reed TM, Browning JE, Blough RI, Vorhees CV, Repaske DR. Genomic structure and chromosome location of the murine PDE1B phosphodiesterase gene. *Mamm Genome*. 1998;9:571-576.
13. Lee HJ, An S, Bae S, Lee JH. Diarylpropionitrile inhibits melanogenesis via protein kinase A/cAMP-response element-binding protein/microphthalmia-associated transcription factor signaling pathway in α-MSH-stimulated B16F10 melanoma cells. *Korean J Physiol Pharmacol*. 2022;26:113-123.

14. Navarro J, Punzón C, Jiménez JL, Fernández-Cruz E, Pizarro A, Fresno M, Muñoz-Fernández MA. Inhibition of phosphodiesterase type IV suppresses human immunodeficiency virus type 1 replication and cytokine production in primary T cells: involvement of NF-kappaB and NFAT. *J Virol*. 1998;72:4712-4720.
15. Guttman-Yassky E, Hanifin JM, Boguniewicz M, Wollenberg A, Bissonnette R, Purohit V, Kilty I, Tallman AM, Zielinski MA. The role of phosphodiesterase 4 in the pathophysiology of atopic dermatitis and the perspective for its inhibition. *Exp Dermatol*. 2019;28:3-10.
16. Crocetti L, Floresta G, Cilibrizzi A, Giovannoni MP. An overview of PDE4 inhibitors in clinical trials: 2010 to early 2022. *Molecules*. 2022;27:4964.
17. Serezani CH, Ballinger MN, Aronoff DM, Peters-Golden M. Cyclic AMP: master regulator of innate immune cell function. *Am J Respir Cell Mol Biol*. 2008;39:127-132.
18. Omar F, Findlay JE, Carfray G, Allcock RW, Jiang Z, Moore C, Muir AL, Lannoy M, Fertig BA, Mai D, Day JP, Bolger G, Baillie GS, Schwiebert E, Klussmann E, Pyne NJ, Ong ACM, Bowers K, Adam JM, Adams DR, *et al*. Small-molecule allosteric activators of PDE4 long form cyclic AMP phosphodiesterases. *Proc Natl Acad Sci U S A*. 2019;116:13320-13329.
19. Damera G, Panettieri RA Jr. Does airway smooth muscle express an inflammatory phenotype in asthma? *Br J Pharmacol*. 2011;163:68-80.
20. Qi P, Wei C, Kou D. Beneficial effects of naringenin and morin on interleukin-5 and reactive oxygen species production in BALB/c mice with ovalbumin-induced asthma. *Korean J Physiol Pharmacol*. 2021;25:555-564.
21. Possa SS, Leick EA, Prado CM, Martins MA, Tibério IF. Eosinophilic inflammation in allergic asthma. *Front Pharmacol*. 2013;4:46.
22. Boswell-Smith V, Spina D, Page CP. Phosphodiesterase inhibitors. *Br J Pharmacol*. 2006;147 Suppl 1(Suppl 1):S252-S257.
23. Zhang YS, Li JD, Yan C. An update on vinpocetine: new discoveries and clinical implications. *Eur J Pharmacol*. 2018;819:30-34.
24. Jeon KI, Xu X, Aizawa T, Lim JH, Jono H, Kwon DS, Abe J, Berk BC, Li JD, Yan C. Vinpocetine inhibits NF-kappaB-dependent inflammation via an IKK-dependent but PDE-independent mechanism. *Proc Natl Acad Sci U S A*. 2010;107:9795-9800.
25. Choi WS, Kang HS, Kim HJ, Lee WT, Sohn UD, Lee JY. Vinpocetine alleviates lung inflammation via macrophage inflammatory protein-1β inhibition in an ovalbumin-induced allergic asthma model. *PLoS One*. 2021;16:e0251012.
26. Kang HS, Song JY, Kim JH, Il Park T, Choi WS, Lee JY. Effects of vinpocetine on atopic dermatitis after administration via three different routes in HR-1 hairless mice. *Pharmazie*. 2022;77:9-13.
27. Jin Y, Jeon H, Le Lam Nguyen T, Kim L, Heo KS. Human milk oligosaccharides 3'-sialyllactose and 6'-sialyllactose attenuate LPS-induced lung injury by inhibiting STAT1 and NF-κB signaling pathways. *Arch Pharm Res*. 2023;46:897-906.
28. Nguyen TLL, Jin Y, Kim L, Heo KS. Inhibitory effects of 6'-sialyllactose on angiotensin II-induced proliferation, migration, and osteogenic switching in vascular smooth muscle cells. *Arch Pharm Res*. 2022;45:658-670.
29. Wollenberg A, Ehmann LM. Long term treatment concepts and proactive therapy for atopic eczema. *Ann Dermatol*. 2012;24:253-260.
30. Kitamura A, Takata R, Aizawa S, Watanabe H, Wada T. A murine model of atopic dermatitis can be generated by painting the dorsal skin with hapten twice 14 days apart. *Sci Rep*. 2018;8:5988.
31. Beheshti R, Halstead S, McKeone D, Hicks SD. Understanding immunological origins of atopic dermatitis through multi-omic analysis. *Pediatr Allergy Immunol*. 2022;33:e13817.
32. Boralevi F, Hubiche T, Léauté-Labrèze C, Saubusse E, Fayon M, Roul S, Maurice-Tison S, Taïeb A. Epicutaneous aeroallergen sensitization in atopic dermatitis infants - determining the role of epidermal barrier impairment. *Allergy*. 2008;63:205-210.
33. Illi S, von Mutius E, Lau S, Nickel R, Grüber C, Niggemann B, Wahn U; Multicenter Allergy Study Group. The natural course of atopic dermatitis from birth to age 7 years and the association with asthma. *J Allergy Clin Immunol*. 2004;113:925-931.
34. Pálsson K, Slagor RM, Flachs EM, Nørreslet LB, Agner T, Ebbehøj NE. Childhood atopic dermatitis is associated with a decreased chance of completing education later in life: a register-based cohort study. *J Eur Acad Dermatol Venereol*. 2021;35:1849-1858.
35. Campanati A, Bianchelli T, Gesuita R, Foti C, Malara G, Micali G, Amerio P, Rongioletti F, Corazza M, Patrizi A, Peris K, Pimpinelli N, Parodi A, Fargnoli MC, Cannavo SP, Pigatto P, Pellacani G, Ferrucci SM, Argenziano G, Cusano F, *et al*; and collaborators. Comorbidities and treatment patterns in adult patients with atopic dermatitis: results from a nationwide multicenter study. *Arch Dermatol Res*. 2022;314:593-603. Erratum in: *Arch Dermatol Res*. 2022;314:605-607.
36. Lodén M. Role of topical emollients and moisturizers in the treatment of dry skin barrier disorders. *Am J Clin Dermatol*. 2003;4:771-788.
37. Hanifin JM, Baghoomian W, Grinich E, Leshem YA, Jacobson M, Simpson EL. The eczema area and severity index-a practical guide. *Dermatitis*. 2022;33:187-192.
38. Yosipovitch G, Papoiu AD. What causes itch in atopic dermatitis? *Curr Allergy Asthma Rep*. 2008;8:306-311.
39. Wang S, Zhu L, Xu Y, Qin Z, Xu A. Salvianolic acid B ameliorates psoriatic changes in imiquimod-induced psoriasis on BALB/c mice by inhibiting inflammatory and keratin markers *via* altering phosphatidylinositol-3-kinase/protein kinase B signaling pathway. *Korean J Physiol Pharmacol*. 2020;24:213-221.
40. Ye N, Cai J, Dong Y, Chen H, Bo Z, Zhao X, Xia M, Han M. A multi-omic approach reveals utility of CD45 expression in prognosis and novel target discovery. *Front Genet*. 2022;13:928328.
41. Waddell LA, Lefevre L, Bush SJ, Raper A, Young R, Lisowski ZM, McCulloch MEB, Muriuki C, Sauter KA, Clark EL, Irvine KM, Pridans C, Hope JC, Hume DA. ADGRE1 (EMR1, F4/80) is a rapidly-evolving gene expressed in mammalian monocyte-macrophages. *Front Immunol*. 2018;9:2246.
42. Tanaka Y, Delaporte E, Dubucquoi S, Gounni AS, Porchet E, Capron A, Capron M. Interleukin-5 messenger RNA and immunoreactive protein expression by activated eosinophils in lesional atopic dermatitis skin. *J Invest Dermatol*. 1994;103:589-592.
43. Amin K. The role of mast cells in allergic inflammation. *Respir Med*. 2012;106:9-14.
44. Dhakal H, Lee S, Kim EN, Choi JK, Kim MJ, Kang J, Choi YA, Baek MC, Lee B, Lee HS, Shin TY, Jeong GS, Kim SH. Gomisin M2 inhibits mast cell-mediated allergic inflammation *via* attenuation of FcεRI-mediated Lyn and Fyn activation and intracellular calcium levels. *Front Pharmacol*. 2019;10:869.